



Synthesis of Sodalite Zeolite from Alkaline Fusion of Kaolin and Crystallization at Low Temperature and Ambient Pressure

Eliomar Pivante Céleri¹ · Carmem Cícera Maria da Silva¹ · Valdemar Lacerda Jr¹ · Audrei Giménez Barañano²

Received: 18 August 2023 / Revised: 3 March 2024 / Accepted: 13 March 2024
© The Author(s) under exclusive licence to Associação Brasileira de Engenharia Química 2024

Abstract

In this study, a sodalite-type zeolite (SOD) was synthesized through the alkaline fusion of kaolin and crystallized under ambient pressure conditions, without the need for autoclaves and high temperatures. The influence of the ratio between fused kaolin and water (g/mL) during crystallization was evaluated. The ratio of fused kaolin with NaOH to water at 1:10 g/mL resulted in the synthesis of zeolite with higher relative crystallinity (70.99%), which was affected by the concomitant formation of therronatrite phase. Additionally, the zeolite showed a Si/Al ratio of 0.95 and Na/Al ratio of 1.00, and the aluminum atoms exhibited a configuration of perfect tetrahedra. Due to the absence of octahedral aluminum in the zeolitic structure and the charge-balancing cations being Na⁺ ions, the zeolite presented itself as a basic solid.

Keywords Zeolite · Alkaline fusion · Sodalite

Introduction

Zeolites are crystalline microporous structures composed of aluminum and silicon oxide. This material exhibits high thermal stability and is utilized as highly efficient adsorbents and catalysts. The presence of micropores imparts zeolites with a high surface area, which is extremely advantageous for various applications, such as water treatment, petroleum cracking, and CO₂ capture, among others (Luna and Schuchardt 2001; Li et al. 2015; Oliveira et al. 2021; He et al. 2021).

Different silicoaluminous minerals, such as kaolin, mineral rich in kaolinite, can be used for zeolite synthesis (Gandhi et al. 2021). For the synthesis of zeolite from kaolin, it is necessary to disrupt its crystalline structure, which is primarily achieved through calcination of kaolin at temperatures between 550 °C and 950 °C. Within this temperature range, the material undergoes dehydroxylation, leading to a change in the aluminum geometry in the gibbsite layer

from octahedral to trigonal pyramidal and tetrahedral. The resulting product is known as metakaolin (Alaba et al. 2015; Sousa et al. 2020).

Crystalline kaolin can be converted into SOD, but it requires hydrothermal treatment at 100 °C for 24 h (Schwanke et al. 2022). Metakaolin is an amorphous material that, in addition to being susceptible to crystallization into a zeolitic structure, is also prone to dealumination when leached in an acidic solution, thereby allowing adjustment of the Si/Al ratio of the material (Abnisa et al. 2021).

The Si/Al ratio of the precursor material influences the type of zeolite obtained. Belviso et al. (2013) demonstrated that a Si/Al ratio close to 1 is favorable for obtaining LTA-type zeolites. Sousa et al. (2020) observed that ratios close to 2 also promote the formation of LTA-type zeolites. However, as this ratio increases to 3 and 4, SOD and FAU-type zeolites start to form.

The three-dimensional structure of SOD zeolite is composed of regular octahedral polyhedra that unite to form cavities known as sodalite or β-cavities. These cavities have an average opening diameter of 2.65 Å, allowing only small molecules such as ammonia (2.50 Å) and water (2.65 Å) to access the interior of these pores. For this reason, SOD zeolites act as molecular sieves (Sousa et al. 2020). SOD zeolites are also known for their excellent selectivity for adsorbing ions such as Cu²⁺, Cd²⁺, Ce³⁺, Pb²⁺, Zn²⁺, and Ni²⁺ (Esaifan et al. 2019; Zhao et al. 2021; Ji and Zhang 2022; Ibrahim et al. 2023).

✉ Valdemar Lacerda Jr
valdemar.lacerda@ufes.br

¹ Núcleo de Competências Em Química Do Petróleo, Universidade Federal Do Espírito Santo, Vitória, ES 29075-910, Brazil

² Centro de Ciências Agrárias E Engenharias, Universidade Federal Do Espírito Santo, Alegre, ES 29500-000, Brazil

The main synthesis method for SOD-type zeolites from metakaolin is the hydrothermal method, where the material is dissolved in an alkaline solution and crystallized in autoclaves (Mamaghani et al. 2022). Table 1 summarizes some of the conditions already explored for the synthesis of SOD zeolites from kaolin.

Hydrothermal synthesis is commonly used to produce SOD-type zeolites from kaolin, yet its high reactivity necessitates autoclaves and elevated temperatures to induce crystallization system pressure (Akinola et al. 2022). However, this method is limited when dealing with materials containing quartz. Moreno-Maroto et al. (2022) found it challenging to disrupt the quartz structure in diatomaceous earth, even after subjecting it to a 24 h hydrothermal treatment at 80 °C using an NaOH solution of 3 mol/L with a solid–liquid ratio of 1 g/10 mL. Tang et al. (2022) investigated optimal conditions for activating kaolin and quartz under hydrothermal conditions. They noted that a 4:1 mass ratio mixture of kaolin and quartz was only disrupted when treated at 200 °C for a minimum of 5 h, using an NaOH solution of 6 mol/L with a solid–liquid ratio of 1 g/20 mL.

In order to obtain a reactive material for the synthesis of zeolites from kaolin, there are few examples that employ the alkaline fusion method to destroy the ore's structure.

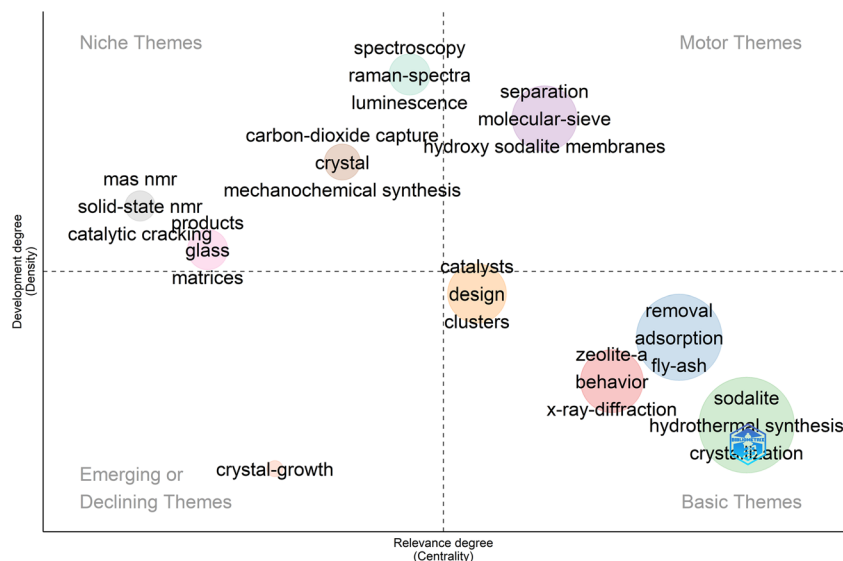
The alkaline fusion method represents an alternative to the hydrothermal treatment method. In this method, the silicoaluminous precursor is fused with potent bases, such as NaOH, at temperatures within the range wherein kaolin converts into metakaolin, specifically between 550 °C and 850 °C. The advantage of this method is that highly thermally stable silicon crystals, such as quartz and mullite, are transformed into water-soluble amorphous compounds, such as Na_2SiO_3 and $\text{Na}_2\text{Al}_2\text{O}_4 \cdot 2.5\text{H}_2\text{O}$, which are reactive for zeolite formation (Ibrahim et al. 2023; Ju et al. 2023).

Bibliometric analysis employing the thematic network approach to investigate the current landscape of research related to SOD zeolite, as depicted in Fig. 1, indicates that hydrothermal synthesis emerges as the predominant mechanism for obtaining SOD zeolite, which was expected, displaying high centrality within the thematic network. Among the addressed applications for this zeolite, it is noted that adsorption (basic theme) and molecule separation (motor theme) are the most explored topics. However, it is noteworthy that the catalytic applications of SOD zeolite have sparked considerable interest in current research, evidenced by the clustering of centralized topics in the diagram (Scarano et al. 2023).

Table 1 Conditions for the synthesis of SOD zeolite from kaolin

Starting material	Initial treatment		Synthesis conditions				Reference
	Calcination (°C)	Time (h)	Temperature (°C)	Time (h)	Alkalizing agent	Si/Al	
Kaolin	600	2	95	6	NaOH	1.16	(Ji and Zhang 2022)
Kaolin residue	700	2	90	72	NaOH	3	(Sousa et al. 2020)
Kaolin with $\text{Er}(\text{NO}_3)_3$	750	2	65	8	NaOH	1.27	(Yuan et al. 2019)
Kaolin	-	-	100	4	NaOH	-	(Prokof'ev et al. 2019)

Fig. 1 Thematic network bibliometric analysis. Search term 'zeolite and sodalite and synthesis', all fields, web of Science database, temporal range 2013–2023



Sodalite-type zeolite was employed by Manique et al. (2017) as a catalyst in biodiesel production, achieving excellent conditions using 4% by weight of the catalyst and a molar ratio of 12:1 (methanol:oil). This resulted in a 95.5% by weight conversion to methyl esters after 2 h of reaction. These results highlight the potential of sodalite zeolite as a low-cost heterogeneous catalyst with applicability on an industrial scale. Another catalytic application using this zeolite was in the preparation of epichlorohydrin from 1,3-dichloropropanol, showing reaction conversion and selectivity superior to 90% (Cui et al. 2020).

In seeking alternatives for synthesizing SOD-type zeolites from kaolin under mild crystallization conditions, without the use of high synthesis temperatures and in the absence of pressure, this study employed a synthesis method based on the alkaline fusion of kaolin with NaOH and crystallization under ambient pressure to obtain SOD zeolite. This approach represents an innovative method prioritizing gentle crystallization conditions. Unlike traditional approaches that require high temperatures and pressure, our method relies on the alkaline fusion of kaolin with NaOH, followed by crystallization under ambient pressure. This strategy offers a promising route for obtaining SOD zeolite, marking a significant advancement by eliminating the need for high temperatures during synthesis, thus rendering it more efficient and accessible for potential industrial applications.

Materials and Methods

Zeolite synthesis

The zeolite synthesis method was inspired by Belviso et al. (2013) who proposed the alkaline fusion synthesis method for obtaining LTA and FAU type zeolites.

The fusion of commercial kaolin (K) occurred through alkaline fusion, where K was mixed in the solid state with NaOH in a ratio of 1:1.2 (w/w) and calcined at 600 °C for 2 h, resulting in the calcined product K-F. Subsequently, K-F was ground using a mortar and pestle and added to distilled water in different proportions (1:5, 1:10, and 1:20 g/mL). After the fusion step, the samples were stirred for 12 h at 25 °C in a Teflon beaker. The beakers were then placed in an oven and kept static at 35 °C for 92 h for zeolite crystallization. Samples were collected at 24 h, and after the 92 h crystallization period, the products were washed with distilled water and dried at 110 °C for 12 h. The samples were named Z-X-Y, where X represents the water ratios (5, 10, and 20), and Y represents the sampling time (24 and 92 h).

The solids were characterized by Fourier Transform Infrared Spectroscopy (FTIR). Spectra were obtained in powder form using an Agilent Cary 600 spectrometer with 100 scans

and a precision of 2 cm⁻¹. X-Ray Diffraction (XRD) was performed using a Bruker D8 diffractometer with CuK α radiation at 1.5406 Å, with settings at 40 kV and 20 mA. Readings were conducted between angles (2 θ) from 5 to 60° with a step size of 0.02 and a scanning rate of 20.min⁻¹. Indexing was performed using the database from the Crystallography Open Database (COD). The diffractograms were employed to determine the material's crystallinity according to Eq. 1.

$$C(\%) = \frac{A_1}{A_t} \times 100 \quad (1)$$

where $C(\%)$ is the percentage of crystallinity of the obtained zeolite, A_1 is the area of the SOD phase diffraction signal, and A_t is the total area.

²⁷Al Nuclear Magnetic Resonance (NMR) spectra were acquired using a Varian-Anilent 400 MHz spectrometer at a 9.4 T field, corresponding to a frequency of 104.16 MHz for ²⁷Al nuclei. Readings were conducted at room temperature with a pulse duration of 1 μ s and a repetition time of 1 s. 800 transients were acquired with a spectral window of 100 kHz and an acquisition time of 20.48 ms. Spectra were referenced using a 1.2 mol.L⁻¹ aqueous solution of aluminum nitrate.

The morphology and chemical composition of the solids were identified by SEM-EDS using a JEOL JSM6610LV microscope, with an adjustable acceleration voltage ranging from 300 V to 30 kV, resolution varying from 3.0 to 15 nm using a tungsten filament, and magnification from 5 to 300,000x. Coupled to the microscope was a Bruker XFlash@ Detector 6110 Energy Dispersive X-ray Spectroscopy (EDS) detector, featuring a 10 mm² analysis area and energy resolution of 121 eV in MnK α , 38 eV in CK α , and 47 eV in FK α (100,000 cps).

Results and Discussion

Zeolite synthesis

K was found to be composed of crystals with a pseudo-hexagonal morphology, forming clusters in the shape of stacked lamellar plates with irregular edges, as shown in Fig. 2. This morphology is characteristic of kaolinite (Cunha et al. 2007; Sousa et al. 2020). The composition was confirmed by XRD analysis in Fig. 1, which revealed a kaolinite rich composition, along with muscovite. Considering the stoichiometric ratio, the Si/Al ratio in kaolinite is equal to 1, which is favorable for the formation of LTA or SOD type zeolites, as observed in previous studies (Zhao et al. 2021; Mamaghani et al. 2022).

The structure of kaolinite was confirmed by FTIR analysis, as shown in Fig. 3. Bands at 3650 and 791 cm⁻¹ were

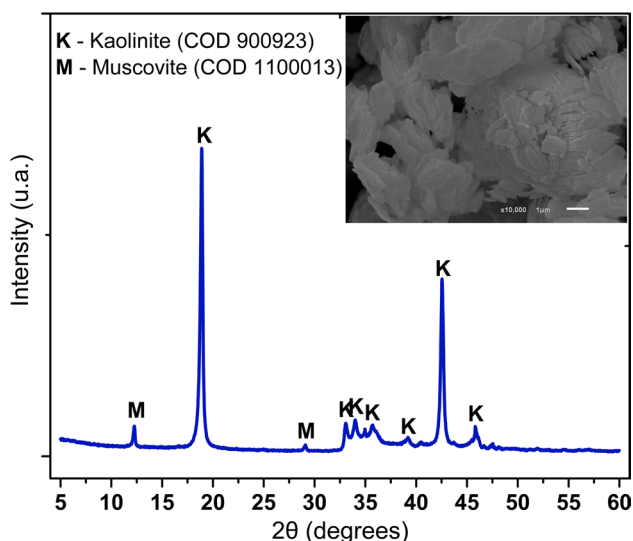


Fig. 2 SEM and XRD of K

observed, which were attributed to different vibrations of the OH group. The band at 1116 cm^{-1} corresponds to the Si–O group that links the layers of kaolinite, and stretching of this same group was also identified in the enplane band at 997 cm^{-1} (Schwanke et al. 2022). The alteration of the crystalline structure of kaolinite mainly occurred due to the dihydroxylation of the gibbsite layer, which contains octahedral aluminum, leading to the formation of sodium aluminosilicate in K-F. The band corresponding to octahedral Al–OH in K at 3650 cm^{-1} disappeared after the alkaline fusion process, and different bands of sodium aluminum silicates were observed between $1120\text{--}800\text{ cm}^{-1}$ in K-F (Khalifah et al. 2019).

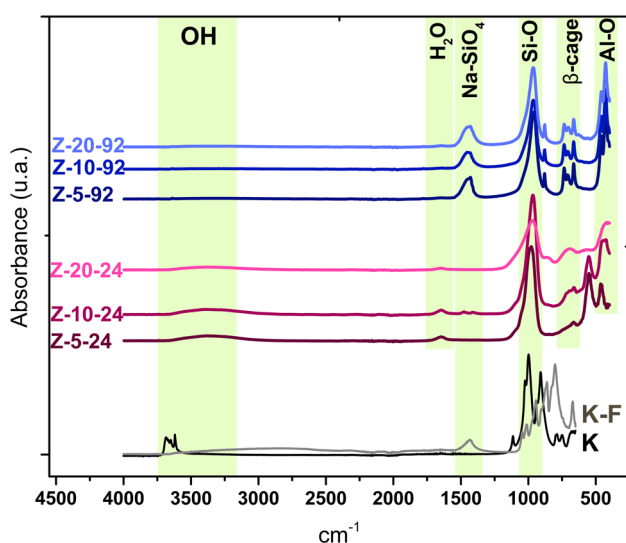


Fig. 3 FTIR spectra of K, K-F and Z-X-Y

After 24 h of crystallization, the FTIR spectra of the formed solids, as shown in Fig. 3, revealed that the various bands of sodium aluminosilicate found in K-F disappeared, giving rise to a single intense band at 967 cm^{-1} , attributed to the stretching of Si–O bonds, and a band at 433 cm^{-1} attributed to the stretching of Al–O bonds, indicating the onset of crystalline growth in an organized structure. Evidence of the formation of a sodalite structure was observed by the characteristic band at 666 cm^{-1} , corresponding to the β -cage oscillations constituting the structure of this SOD zeolite (Klima et al. 2022). In addition to these bands, there is a broad band near 3300 cm^{-1} related to the stretching of OH bonds, which can be attributed to the presence of Si(Al)-OH species or adsorbed water in the Si–O–Si(Al) bridging, generating a band near 1630 cm^{-1} , also observed.

After 92 h of crystallization, as depicted in Fig. 3, the bands at 662 and 735 cm^{-1} , attributed to the β -cage structures, were well-defined, indicating the absence of adsorbed water or the presence of Si(Al)-OH sites. This was evidenced by the lack of a broad band near 3000 cm^{-1} . A more intense band at 1442 cm^{-1} and a less intense band at 870 cm^{-1} were observed, attributed to vibrations present in sodium orthosilicate (Na_4SiO_4) (Ellerbrock et al. 2022).

The confirmation of the sodalite structure in the zeolites was conducted through XRD analysis, as illustrated in Fig. 4. In all cases, after 92 h of crystallization, the products synthesized from different ratios of K-F to water resulted in the formation of the SOD-type zeolite phase, which was the predominant phase formed due to the higher intensity of the signals observed in the diffractograms. Additionally, it can be observed in Fig. 4 that after 24 h of crystallization, the diffractograms showed an absence of diffraction peaks, indicating a slower crystallization kinetics compared to the results reported by Esaifan et al. (2019) where the sodalite phase was obtained

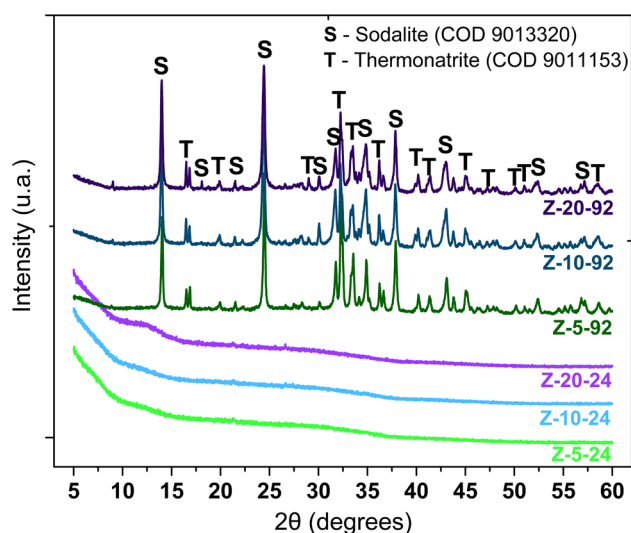


Fig. 4 XRD diffractograms of the products after 24 and 92 h of crystallization

in 6 h at 160 °C hydrothermal. This finding suggests a significant influence of temperature on the crystallization kinetics in the synthesis of SOD zeolite.

The crystallinity of SOD zeolites, influenced by the K-F:water ratio, was crucial for the therronatrite phase formation. Higher crystallinity, approximately 70%, was observed in syntheses with ratios of 1:10 and 1:20, while a synthesis with a ratio of 1:5 showed a crystallinity of 57.87%. These synthesis parameters played a pivotal role in determining the resulting SOD zeolites crystallinity.

Temperature and crystallization duration were noted by Khalifah et al. (2019) to significantly impact both the crystallinity and size of the obtained SOD crystals. Achieving SOD zeolites with over 70% crystallinity through hydrothermal treatment was reported solely by Ji and Zhang (2022) when a temperature of 75 °C. In contrast, García-Villén et al. (2018) attained SOD with 35% crystallinity using hydrothermal treatment at 150 °C for 12 h.

Furthermore, the crystallinity of SOD zeolites derived from fused kaolin was shown to be affected by the K-F:water ratio during crystallization, an aspect previously unexplored for this zeolite. Bai et al. (2018) demonstrated an increase in FAU zeolite crystallinity from 20.64% to 76.22% with an increase in the fused shale to NaOH to water ratio from 1:3 (g/mL) to 1:4 (g/mL). However, a further increase from 1:4 to 1:5 (g/mL) led to a decrease in crystallinity from 76.22% to 29.41%.

The authors Bai et al. (2018) attributed this phenomenon to the concentration of hydroxyl ions dispersed in the solution. At low alkalinity (high solid–liquid ratio), the concentration of hydroxyl ions is insufficient to depolymerize the starting material and form the zeolitic nuclei necessary for crystallization. At high alkalinity (low sol-id-liquid ratio), the high concentration of hydroxyl ions solubilizes the formed nuclei, impeding crystal growth.

Despite the similar crystallinity observed between Z-10–92 and Z-20–92, the choice of a K-F:water ratio of 1:10 is deemed more beneficial as it mitigates the generation of synthesis effluents by using a reduced amount of water. This synthesis condition is suggested as the most effective for obtaining ambient-pressure crystallized SOD zeolite. Therefore, we opted to characterize only this obtained zeolite, considering it as the most efficient and sustainable option for the process.

One of the main parameters impacting zeolite synthesis is the Si/Al ratio of precursor materials, which influences the resulting zeolite type and morphology. Consequently, this affects their properties and crystallinity. Generally, the closer

the Si/Al ratio of the precursors is to the desired zeolite, the fewer pretreatment steps and additional materials are needed during synthesis (Bieseki et al. 2013).

SOD zeolite, obtained through hydrothermal treatment, has been reported in previous studies with different Si/Al ratios: 1.42 when crystallized at 95 °C for 24 h (Franus et al. 2014); 1.30 after 48 h at 110 °C (Tauanov et al. 2019) and 1.02 after 6 h at 120 °C (Sánchez-Hernández et al. 2016). In this study, where crystallization occurred at ambient pressure for 92 h, the Si/Al ratio was 0.95, as shown in Table 2, and the synthesis success is linked to the kaolin's Si/Al ratio close to that of the zeolite, which was 1.22.

The presence of aluminum in zeolite structures is crucial for the versatility of their applications, as this component plays a fundamental role in their ion exchange properties and catalytic activity. However, it's important to note that an excessive concentration of aluminum can significantly reduce crystallinity, as this excess may lead to the hydrolysis of zeolitic nuclei during the crystallization step (Ye et al. 2022). Zeolites with low silica content, such as SOD, have a Si/Al ratio close to 1, and due to the high density of structural aluminum, an excess of compensating ions is required to balance the zeolite's charge. As observed, the Na/Al ratio is 1.00, consistent with the Si/Al ratio of 0.95.

Sodalite-type zeolites are found in clusters with irregular particles ranging in size from 0.5 to 1 µm (Prokof'ev et al. 2019). The SEM–EDS images, Figs. 5-A and 5-B, reveal that the Z-10–92 product consists of agglomerated particles with dimensions smaller than 1 µm, attributed to the presence of the zeolitic phase in the sample. Besides these clusters, potassium crystals can be observed in Fig. 5-A; these crystals may have formed due to the presence of potassium in the composition of K, and silicon in Fig. 5-B.

Zeolites can possess both Brønsted and Lewis acid sites. Brønsted sites are associated with tetrahedrally coordinated aluminum with a negative charge, balanced by H⁺ ions bonded to an oxygen atom at the tetrahedral edge (AlO₄)⁻. On the other hand, Lewis sites are attributed to octahedrally coordinated aluminum, which can occupy different positions within the zeolite structure (Ravi et al. 2020, 2021).

The relationship between Lewis acidity and aluminum structure in mordenite zeolite was examined by Ravi et al. (2019) The evidence showed that the amount of octahedrally coordinated aluminum in the hydrated samples is directly related to the number of Lewis acid sites present. These Lewis acid sites are particularly relevant when charge balancing occurs through protons.

Table 2 Chemical composition of K and Z-10–92 by EDS

Material	Percent mass (%)				
	Si	Al	Na	K	Fe
K	51.87 (±0.5)	42.49 (±0.5)	4.11 (±2.3)	0.91 (±2.3)	0.53 (±1.3)
Z-10–92	31.64 (±0.9)	33.21 (±1.1)	33.26 (±1.7)	1.31 (±0.1)	-

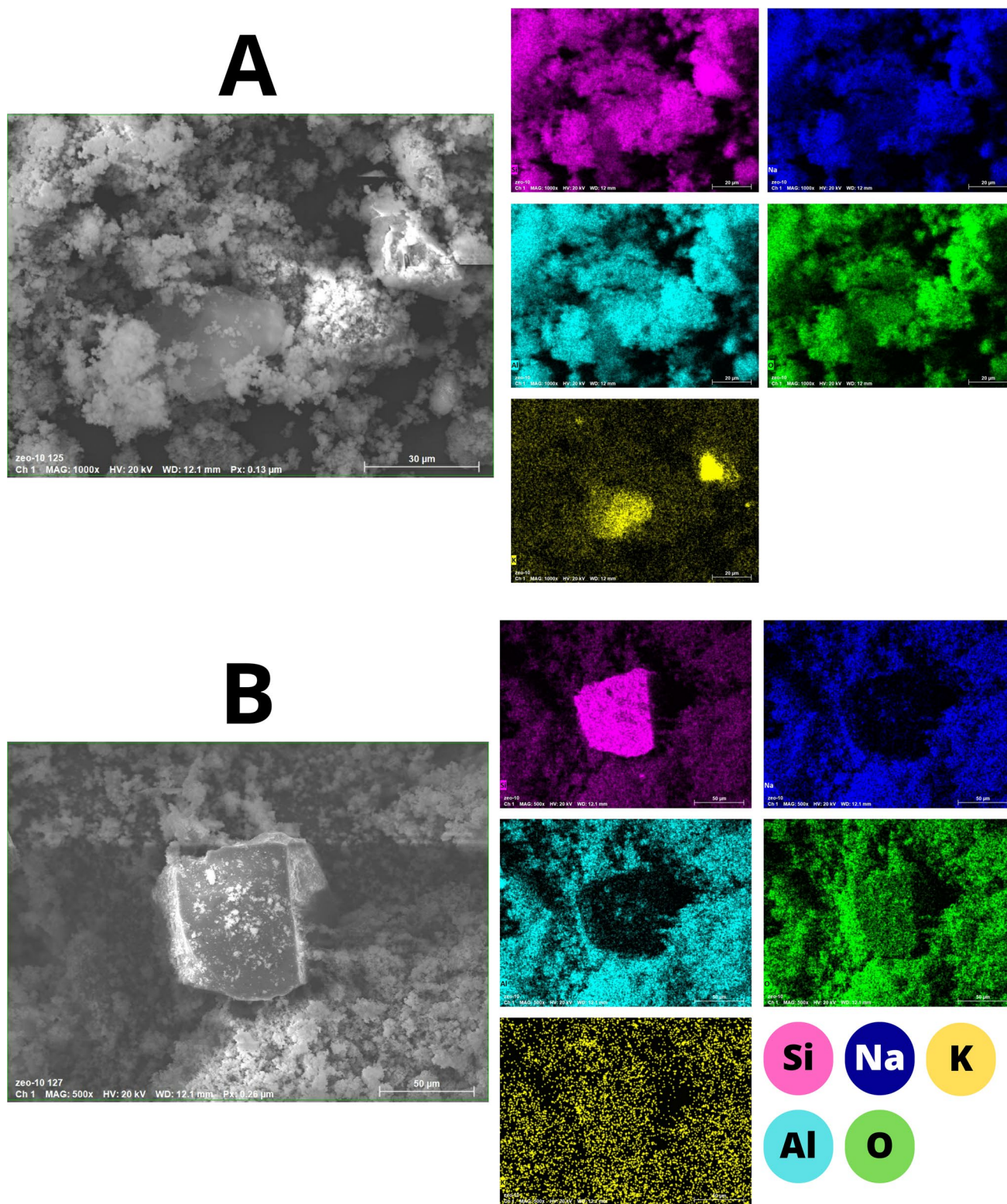
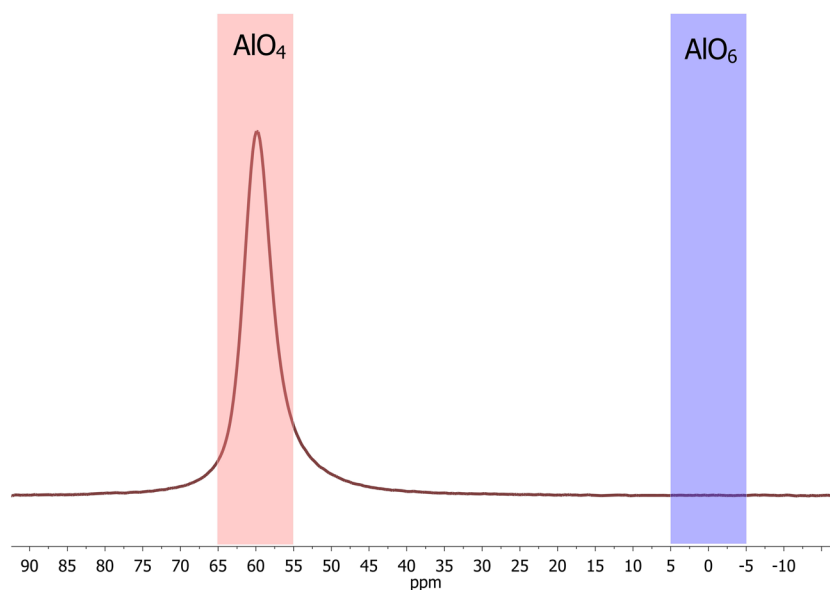


Fig. 5 SEM-EDS of Z-10-92

As demonstrated in the FTIR analysis, as shown in Fig. 3, and confirmed by SEM-EDS images, Figs. 5-A and 5-B, the obtained zeolite was in the sodium form and lacked bands

related to OH, indicating the absence of Brønsted acid sites. The absence of Lewis acid sites was confirmed by ^{27}Al NMR in the sodium state, as depicted in Fig. 6, where the

Fig. 6. ^{27}Al NMR spectrum of the Z-10



absence of octahedral aluminum at 0 ppm and the presence of a strong signal at 58 ppm, characteristic of tetrahedral aluminum, were observed (Walkley and Provis 2019).

The synthesis of SOD zeolites at low temperatures (35 °C) without the use of autoclaves, as demonstrated in this study, represents a significant advancement in reducing the production costs of these materials. This approach eliminates the need for autoclaves, substantially reducing the energy required for crystallization. It also utilizes, for the fusion step, a temperature like that used for transforming kaolin into metakaolin, the traditional method employed in the hydrothermal route using autoclaves. Additionally, the alkaline fusion method can amorphized high thermally stable silicon structures, such as quartz. This enables the utilization of kaolin waste rich in this mineral for synthesis, opening new avenues to obtain SOD zeolites with higher crystallinity. This innovation expands the possibilities for future research to explore and enhance the synthesis parameters of these zeolites.

Conclusions

The results obtained in this study highlight the promising feasibility of synthesizing SOD-type zeolites from alkaline fusion of kaolin, conducted under low-temperature and ambient-pressure conditions. This emerging methodology provides an economical and effective approach to obtaining this material without relying on equipment such as autoclaves. The findings indicated that the zeolite with the highest crystallinity was produced using a K-F:water ratio of 1:10, achieving 70.99% crystallinity, and demonstrated its basic character through the presence of Na^+ cations as charge compensators and the

absence of octahedral aluminum in the zeolite structure. This innovative method represents a significant step in zeolite research, offering an accessible and potentially scalable route for the production of these technologically relevant materials.

Acknowledgements The authors would like to thank the Fundação de Amparo a Pesquisa do Espírito Santo (FAPES) for the financial support provided through a master's scholarship. They also express their gratitude to the Characterization and X-ray Diffractometry Laboratories at the Núcleo de Competências em Química do Petróleo (LabPetro) of the Universidade Federal do Espírito Santo (UFES) for performing the FTIR and XRD analyses, respectively. Additionally, they acknowledge the Carlos Alberto Redins Cellular Ultrastructure Laboratory (LUC-CAR/UFES) for conducting the SEM-EDX analysis.

Data availability The data used in this study is available upon request to the corresponding author.

Declarations

The authors have no financial or proprietary interests in any material discussed in this article.

References

- Abnisa F, Sanni SE, Alaba PA (2021) Comparative study of catalytic performance and degradation kinetics of biodiesels produced using heterogeneous catalysts from kaolinite. *J Environ Chem Eng* 9:105569. <https://doi.org/10.1016/j.jece.2021.105569>
- Akinola TE, Bonilla Prado PL, Wang M (2022) Experimental studies, molecular simulation and process modelling\simulation of adsorption-based post-combustion carbon capture for power plants: A state-of-the-art review. *Appl Energy* 317:119156. <https://doi.org/10.1016/j.apenergy.2022.119156>
- Alaba PA, Sani YM, Ashri Wan Daud WM (2015) Kaolinite properties and advances for solid acid and basic catalyst synthesis. *RSC Adv* 5:101127–101147. <https://doi.org/10.1039/C5RA18884A>

- Bai S, Zhou L, Chang Z, Zhang C, Chu M (2018) Synthesis of Na-X zeolite from Longkou oil shale ash by alkaline fusion hydrothermal method. *Carbon Resources Conversion* 1:245–250. <https://doi.org/10.1016/j.crcon.2018.08.005>
- Belviso C, Cavalcante F, Lettino A, Fiore S (2013) A and X-type zeolites synthesised from kaolinite at low temperature. *Appl Clay Sci* 80–81:162–168. <https://doi.org/10.1016/j.clay.2013.02.003>
- Bieseki L, Ribeiro DB, Sobrinho EV, Melo DMA, Pergher SBC (2013) Synthesis of zeolites using silico-aluminous residue from the lithium extraction process. <https://doi.org/10.1590/S0366-69132013000300018>
- Cui L, Han R, Yang L, Wu Y, Pei R, Li F (2020) Synthesis and characterization of mesoporous sodalite and investigation of the effects of inorganic salts on its structure and properties. *Microporous Mesoporous Mater* 306:110385. <https://doi.org/10.1016/j.micromeso.2020.110385>
- Cunha FOD, Torem ML, D'Abreu JC (2007) A influência do pH na reologia de polpas de caulim. *Rem Rev Esc Minas* 60:505–511. <https://doi.org/10.1590/S0370-44672007000300011>
- Ellerbrock R, Stein M, Schaller J (2022) Comparing amorphous silica, short-range-ordered silicates and silicic acid species by FTIR. *Sci Rep* 12:11708. <https://doi.org/10.1038/s41598-022-15882-4>
- Esaifan M, Warr LN, Grathoff G, Meyer T, Schafmeister M-T, Kruth A, Testrich H (2019) Synthesis of Hydroxy-Sodalite/Cancrinite Zeolites from Calcite-Bearing Kaolin for the Removal of Heavy Metal Ions in Aqueous Media. *Minerals* 9:484. <https://doi.org/10.3390/min9080484>
- Franus W, Wdowin M, Franus M (2014) Synthesis and characterization of zeolites prepared from industrial fly ash. *Environ Monit Assess* 186:5721–5729. <https://doi.org/10.1007/s10661-014-3815-5>
- Gandhi D, Bandyopadhyay R, Soni B (2021) Zeolite Y from kaolin clay of Kachchh, India: Synthesis, characterization and catalytic application. *J Indian Chem Soc* 98:100246. <https://doi.org/10.1016/j.jics.2021.100246>
- García-Villén F, Flores-Ruiz E, Verdugo-Escamilla C, Huertas FJ (2018) Hydrothermal synthesis of zeolites using sanitary ware waste as a raw material. *Appl Clay Sci* 160:238–248. <https://doi.org/10.1016/j.clay.2018.02.004>
- He Y, Tang S, Yin S, Li S (2021) Research progress on green synthesis of various high-purity zeolites from natural material-kaolin. *J Clean Prod* 306:127248. <https://doi.org/10.1016/j.jclepro.2021.127248>
- Ibrahim AH, Lyu X, ElDeeb AB (2023) Synthesized Zeolite Based on Egyptian Boiler Ash Residue and Kaolin for the Effective Removal of Heavy Metal Ions from Industrial Wastewater. *Nanomaterials* 13:1091. <https://doi.org/10.3390/nano13061091>
- Ji B, Zhang W (2022) Adsorption of cerium (III) by zeolites synthesized from kaolinite after rare earth elements (REEs) recovery. *Chemosphere* 303:134941. <https://doi.org/10.1016/j.chemosphere.2022.134941>
- Ju T, Han S, Meng F, Lin L, Li J, Chen K, Jiang J (2023) Porous silica synthesis out of coal fly ash with no residue generation and complete silicon separation. *Front Environ Sci Eng* 17:112. <https://doi.org/10.1007/s11783-023-1712-2>
- Khalifah SN, Cahyawati M, Cahyani DKD, Arifah A, Prasetyo A (2019) Synthesis of Sodalite from Indonesian Kaolin with Conventional and Alkali Fusion Method. *IOP Conf Ser: Mater Sci Eng* 578:012006. <https://doi.org/10.1088/1757-899X/578/1/012006>
- Klima KM, Schollbach K, Brouwers HJH, Yu Q (2022) Enhancing the thermal performance of Class F fly ash-based geopolymer by sodalite. *Constr Build Mater* 314:125574. <https://doi.org/10.1016/j.conbuildmat.2021.125574>
- Li J, Zeng X, Yang X, Wang C, Luo X (2015) Synthesis of pure sodalite with wool ball morphology from alkali fusion kaolin. *Mater Lett* 161:157–159. <https://doi.org/10.1016/j.matlet.2015.08.058>
- Luna FJ, Schuchardt U (2001) Modificação de zeólitas para uso em catálise. *Quím Nova* 24:885–892. <https://doi.org/10.1590/S0100-40422001000600027>
- Mamaghani FAA, Salem A, Salem S (2022) Role of aluminum resource in conversion of bentonite into low silica-based zeolites via fusion technology. *Mater Lett* 318:132168. <https://doi.org/10.1016/j.matlet.2022.132168>
- Manique MC, Lacerda LV, Alves AK, Bergmann CP (2017) Biodiesel production using coal fly ash-derived sodalite as a heterogeneous catalyst. *Fuel* 190:268–273. <https://doi.org/10.1016/j.fuel.2016.11.016>
- Moreno-Maroto JM, Alonso-Azcárate J, Martínez-García C, Romero M, López-Delgado A, Cotes-Palomino T (2022) Zeolitization of Diatomite Residues by a Simple Method. *Appl Sci* 12:10977. <https://doi.org/10.3390/app122110977>
- Oliveira E, Alves C, França A, Nascimento R, Sasaki J, Loiola A (2021) Zeólita na sintetizada sobre fibra de vidro como estratégia para otimização do abrandamento de águas duras. *Quím Nova*. <https://doi.org/10.21577/0100-4042.20170797>
- Prokof'ev VY, Gordina NE, Borisova TN, Shamanaeva NV (2019) Study of the kinetics of water desorption on binder-free pellets of SOD and LTA zeolites using model-free isoconversion analyzes. *Microporous Mesoporous Mater* 280:116–123. <https://doi.org/10.1016/j.micromeso.2019.01.028>
- Ravi M, Sushkevich VL, van Bokhoven JA (2019) Lewis Acidity Inherent to the Framework of Zeolite Mordeinite. *J Phys Chem C* 123:15139–15144. <https://doi.org/10.1021/acs.jpcc.9b03620>
- Ravi M, Sushkevich VL, van Bokhoven JA (2020) Towards a better understanding of Lewis acidic aluminium in zeolites. *Nat Mater* 19:1047–1056. <https://doi.org/10.1038/s41563-020-0751-3>
- Ravi M, Sushkevich VL, van Bokhoven JA (2021) On the location of Lewis acidic aluminum in zeolite mordeinite and the role of framework-associated aluminum in mediating the switch between Brønsted and Lewis acidity. *Chem Sci* 12:4094–4103. <https://doi.org/10.1039/D0SC06130A>
- Sánchez-Hernández R, López-Delgado A, Padilla I, Galindo R, López-Andrés S (2016) One-step synthesis of NaP1, SOD and ANA from a hazardous aluminum solid waste. *Microporous Mesoporous Mater* 226:267–277. <https://doi.org/10.1016/j.micromeso.2016.01.037>
- Scarano A, Aria M, Mauriello F, Riccardi MR, Montella A (2023) Systematic literature review of 10 years of cyclist safety research. *Accid Anal Prev* 184:106996. <https://doi.org/10.1016/j.aap.2023.106996>
- Schwanke AJ, Silveira DR, Saorin Puton BM, Cansian RL, Bernardo-Gusmão K (2022) Sustainable conversion of Brazilian Amazon kaolin mining waste to zinc-based Linde Type A zeolites with antibacterial activity. *J Clean Prod* 338:130659. <https://doi.org/10.1016/j.jclepro.2022.130659>
- Sousa BB, Rego JAR, Brasil DSB, Martelli MC (2020) Síntese e caracterização de zeólita tipo sodalita obtida a partir de resíduo de caulim. *Cerâmica* 66:404–412. <https://doi.org/10.1590/0366-69132020663802758>
- Tang L-J, Xie X-Z, Huang Y-X, Pan Y, Mi J-X (2022) Phase diagram for hydrothermal alkali activation of kaolin and quartz: Optimal digestion for the synthesis of zeolites. *Mater Chem Phys* 290:126570. <https://doi.org/10.1016/j.matchemphys.2022.126570>
- Tauanov Z, Tsakiridis PE, Shah D, Inglezakis VJ (2019) Synthetic sodalite doped with silver nanoparticles: Characterization and mercury (II) removal from aqueous solutions. *Journal of Environmental Science and Health, Part A* 54:951–959. <https://doi.org/10.1080/10934529.2019.1611129>
- Walkley B, Provis JL (2019) Solid-state nuclear magnetic resonance spectroscopy of cements. *Materials Today Advances* 1:100007. <https://doi.org/10.1016/j.mtadv.2019.100007>
- Ye T, Chen Z, Chen Y, Xie H, Zhong Q, Qu H (2022) Green synthesis of ZSM-5 zeolite for selective catalytic reduction of NO via

template-free method from tailing residue. *J Environ Chem Eng* 10:107766. <https://doi.org/10.1016/j.jece.2022.107766>

Yuan W, Kuang J, Yu M, Huang Z (2019) Effect of $\text{Er}(\text{NO}_3)_3$ on thermal activation of kaolinite and alkaline reaction behavior of metakaolin. *Powder Technol* 354:727–733. <https://doi.org/10.1016/j.powtec.2019.06.042>

Zhao D, Armutlulu A, Chen Y, Wang Y, Xie R (2021) Highly efficient removal of $\text{Cu}(\text{II})$ using mesoporous sodalite zeolite produced from industrial waste lithium-silicon-fume via reactive oxidation species route. *J Clean Prod* 319:128682. <https://doi.org/10.1016/j.jclepro.2021.128682>

Statement: During the preparation of this work the authors used *ChatGPT*, developed by *OpenAI* in order to improve language translation. After using this tool/service, the authors reviewed and

edited the content as needed and takes full responsibility for the content of the publication.

Publisher's Note Springer Nature remains neutral with regard to jurisdictional claims in published maps and institutional affiliations.

Springer Nature or its licensor (e.g. a society or other partner) holds exclusive rights to this article under a publishing agreement with the author(s) or other rightsholder(s); author self-archiving of the accepted manuscript version of this article is solely governed by the terms of such publishing agreement and applicable law.